Effect of Cations on the Structure and Electrocatalytic Response of Polyoxometalate-Based Coordination Polymers

William Salomon, Grégoire Paille, Maria Gomez-Mingot, Pierre Mialane, Jérôme Marrot, Marc Roch-Marchal, Grégory Nocton, Caroline Mellot-Draznieks, Marc Fontecave, Anne Dolbecq

▶ **To cite this version:**

William Salomon, Grégoire Paille, Maria Gomez-Mingot, Pierre Mialane, Jérôme Marrot, et al.. Effect of Cations on the Structure and Electrocatalytic Response of Polyoxometalate-Based Coordination Polymers. Crystal Growth & Design, 2017, 10.1021/acs.cgd.6b01600 . hal-01494047

HAL Id: hal-01494047

https://hal.sorbonne-universite.fr/hal-01494047

Submitted on 22 Mar 2017

HAL is a multi-disciplinary open access archive for the deposit and dissemination of scientific research documents, whether they are published or not. The documents may come from teaching and research institutions in France or abroad, or from public or private research centers.

L'archive ouverte pluridisciplinaire **HAL**, est destinée au dépôt et à la diffusion de documents scientifiques de niveau recherche, publiés ou non, émanant des établissements d'enseignement et de recherche français ou étrangers, des laboratoires publics ou privés.

Effect of Cations on the Structure and Electrocatalytic Response of Polyoxometalate-Based Coordination Polymers

William Salomon,[†] Grégoire Paille,[†,‡] Maria Gomez-Mingot,[*,‡] Pierre Mialane,[†] Jérôme Marrot,[†] Catherine Roch-Marchal,[†] Gregory Nocton,[§] Caroline Mellot-Draznieks,[‡] Marc Fontecave,[*,‡] and Anne Dolbecq[*,†]

[†] Institut Lavoisier de Versailles, UMR 8180 CNRS, Université Paris Saclay, Université de Versailles Saint-Quentin en Yvelines, 45 Avenue des Etats-Unis, 78035 Versailles Cedex, France.

[‡] Laboratoire de Chimie des Processus Biologiques, UMR 8229 CNRS, Collège de France, Université Paris 6, 11 Place Marcelin Berthelot, 75231 Paris Cedex 05, France.

§ Laboratoire de Chimie Moléculaire, CNRS, Ecole Polytechnique, 91128 Palaiseau Cedex, France

ABSTRACT: A series of six hybrid polymers based on the mixed-valent {ε-$PMo^{V}_{8}Mo^{VI}_{4}O_{40}Zn_4$} (εZn) Keggin unit have been synthesized under hydrothermal conditions using tritopic (1,3,5-benzenetricarboxylate (trim) or benzenetribenzoate (BTB)) or ditopic (4,4'-biphenyldicarboxylate (biphen)) linkers and $[M(bpy)_3]^{2+}$ (M = Co, Ru) complexes as charge-compensating cations. $(TBA)_2[Co(C_{10}H_8N_2)_3][PMo_{12}O_{37}(OH)_3Zn_4](C_{27}H_{15}O_6)_{4/3}\cdot 1.5\ C_{27}H_{18}O_6\cdot 24H_2O$ (**Co-ε(BTB)$_{4/3}$**) has a 3D framework with two interpenetrated networks and is isostructural to $(TBA)_4[PMo_{12}O_{37}(OH)_3Zn_4](C_{27}H_{15}O_6)_{4/3}\cdot 1.5C_{27}H_{18}O_6\cdot 8H_2O$ (**ε(BTB)$_{4/3}$**). In **Co-ε(BTB)$_{4/3}$** two tetrabutylammonium (TBA^+) cations over the four present in **ε(BTB)$_{4/3}$** are replaced by one $[Co(bpy)_3]^{2+}$ complex. $[Co(C_{10}H_8N_2)_3][PMo_{12}O_{37}(OH)_3Zn_4](C_9H_3O_6)Co(C_{10}H_8N_2)_4(H_2O)\cdot 16H_2O$ (**Co-ε(trim)(bpy)$_2$**) is a 1D coordination polymer with two types of Co^{II}-containing complexes, one covalently attached to the 1D chains and the other located in the voids as counter-ion. $[Ru(C_{10}H_8N_2)_3]_4[PMo_{12}O_{38}(OH)_2Zn_4]_2(C_9H_3O_6)_2\cdot 42H_2O$ (**Ru-ε$_2$(trim)$_2$**) and $[Ru(C_{10}H_8N_2)_3]_3[PMo_{12}O_{37}(OH)_3Zn_4Cl]_2(C_{14}H_8O_4)_2\cdot 24H_2O$ (**Ru-ε$_2$(biphen)$_2$**) contain dimeric $(εZn)_2$ units linked by dicarboxylate linkers and both have $[Ru(bpy)_3]^{2+}$ counter-cations. **Ru-ε$_2$(trim)$_2$** has a 3D framework while **Ru-ε$_2$(biphen)$_2$** is only 2D due to the presence of chloride ions on 1/4 of the Zn^{II} ions. $[P(C_6H_5)_4]_6[PMo_{12}O_{37}(OH)_3Zn_4]_2(C_9H_3O_6)_2\cdot 18H_2O$ (**PPh$_4$-ε$_2$(trim)$_2$**) is isostructural to **Ru-ε$_2$(trim)$_2$**. These insoluble compounds entrapped in carbon paste electrodes exhibit electrocatalytic activity for the hydrogen evolution reaction (HER). Effects of their structure and of the nature of the counter-ions on the activity are studied. For the first time different POM-based coordination polymers are compared for catalytic H_2 production using controlled potential electrolysis. This study shows that the nature of the counter-cation has a strong effect on the electrocatalytic activity of the compounds.

INTRODUCTION

Coordination polymers are hybrid organic-inorganic materials built of inorganic secondary building units (clusters, chains or layers) assembled by coordination bonds between metal ions and polytopic organic linkers, metal organic frameworks (MOFs) being defined as porous coordination networks.[1] These last years, a new class of coordination polymers has emerged where the inorganic building unit is constituted by a polyoxometalate (POM) as an alternative to metal ions.[2] Polyoxometalates are soluble anionic metal oxide clusters of d-block transition metals in high oxidation states (usually W^{VI}, $Mo^{V,VI}$, $V^{IV,V}$)[3] and exhibit properties that can be exploited in many fields ranging from magnetism, medicine, photochromism to catalysis.[4] POMs can be connected to each other via M-O-M' (M, M' = transition metal) linkages.[5] They can also act as building units of hybrid materials, the connection being ensured by transition metal complexes[6,7] or bridging organic ligands.[8] Such polyoxometalate-based coordination polymers are sometimes called POMOFs.[2,9] POMs are often considered as electron reservoirs and their catalytic redox activity has attracted a lot of interest in recent years.[10] Several studies have shown the potentialities of molecular POMs as electrocatalysts for hydrogen evolution reaction (HER),[11] NOx reduction,[12] oxygen reduction,[13] and water oxidation.[14]

Among these reactions, HER is one of the most extensively studied electrochemical processes, as H_2 may provide an alternative to hydrocarbon fuels due to its high energy content and environmentally benign nature. While platinum is known as a very efficient electrocatalyst for the reduction of protons, great efforts are now devoted to the replacement of this noble metal by cheaper and more abundant materials. Besides POMs, transition metal chalcogenides,[15] nitrides and carbides[16] as well as molecular catalysts based on non-noble metal ions,[17] such as molybdenum,[18] iron,[19] cobalt[20] or nickel,[21] have thus been reported as rather efficient homogeneous cathode catalysts for the HER. However, homogeneous

catalysis also suffers from several drawbacks such as limited stability and uneasy catalyst recovery and recycling. Recent reports thus focussed on the heterogeneization of active molecular catalysts via incorporation into the framework of coordination polymers, including metal organic frameworks.[22] Although these materials offer several advantages, there have been only few reports on POM-based coordination polymers.[23] Actually, they are synthesized in water in a one-step procedure, they contain abundant and non-toxic metals and operate in water at low overpotentials.[23a,b]

In the context of our studies on POMOFs, we have selected the ε-Keggin POM unit, {ε-$PMo^{V}_{8}Mo^{VI}_{4}O_{40-x}(OH)_{x}Zn_{4}$} ($0 \leq x \leq 4$, noted εZn, Figure 1a), as it is particularly attractive for the construction of POM-based coordination polymers. In this mixed-valent POM, the electrons of the eight Mo^{V} ions are localized in four Mo^{V}-Mo^{V} bonds. The negatively charged [ε-$PMo^{V}_{8}Mo^{VI}_{4}O_{40}$]$^{11-}$ Keggin core is stabilized by Zn^{II} capping ions and by protons located on bridging oxygen atoms. It thus presents the advantage of having four Zn^{II} ions grafted at its surface in a tetrahedral arrangement available for coordinating ditopic linkers like 1,4-benzenedicarboxylate (bdc),[24] 1,3-benzenedicarboxylate,[25] imidazole,[26] 2-(2-pyridyl)-imidazole,[27] 4,4'-bipyridine,[28] or the tritopic 1,3,5-benzenetricarboxylate (trim) linkers.[23a] We have also recently extended this family of POMOFs materials by using a mixture of two ligands, benzimidazole and a di- or a tri-carboxylic acid.[23b]

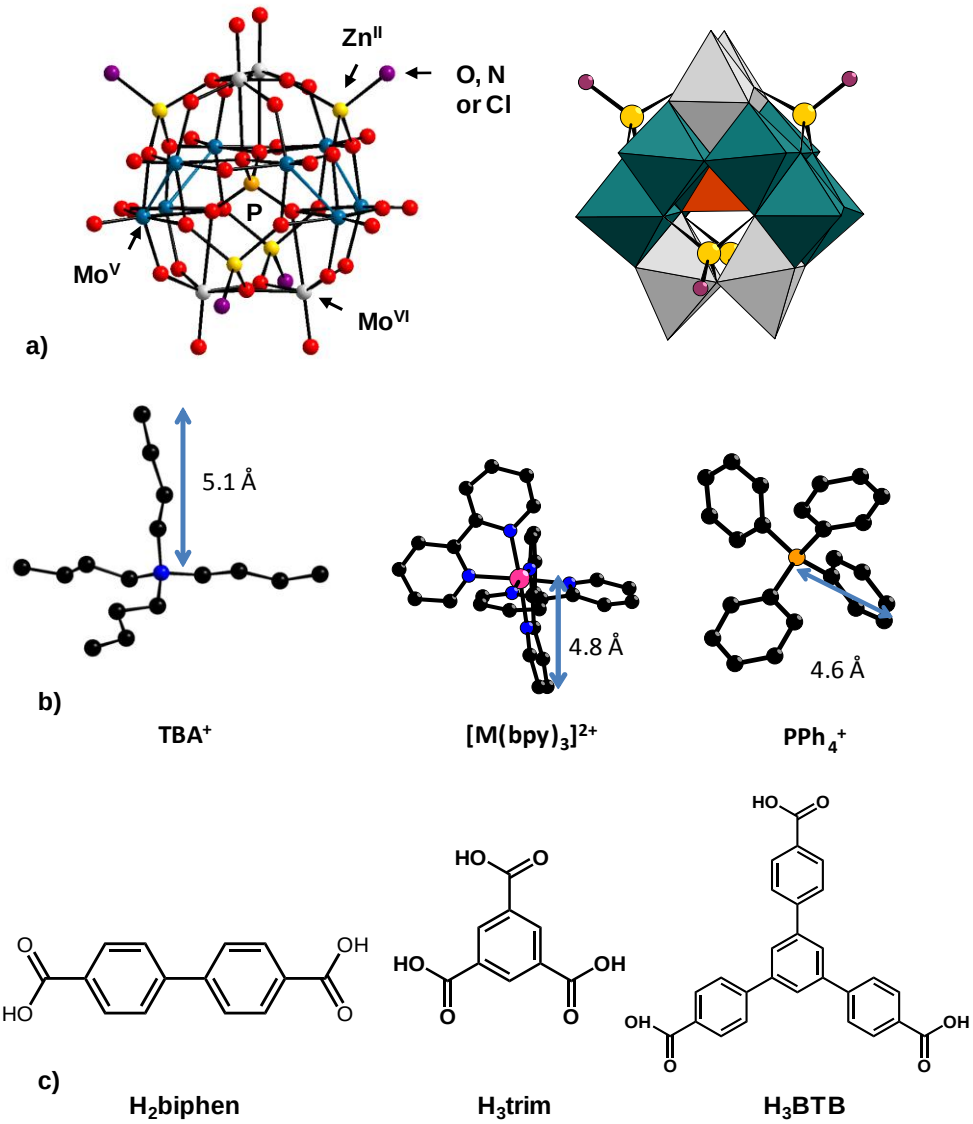

Figure 1. a) Ball and stick and polyhedral representations of the monomeric {ε-$PMo^{V}_{8}Mo^{VI}_{4}O_{40-x}(OH)_{x}Zn_{4}$} Keggin building unit; b) representation of the counter-ions with their approximate dimensions, H atoms have been omitted for clarity; red spheres: O, blue spheres : N, black spheres : C, pink sphere: M (M = Co, Ru), orange spheres : P; c) formula of the carboxylic acids used in this study: biphenyl-4,4'-dicarboxylic acid (H_2biphen), 1,3,5-benzenetricarboxylic acid (H_3trim) and 1,3,5-tris(4-carboxyphenyl)benzene (H_3BTB).

In almost all the ε-Keggin based coordination polymers, tetrabutylammonium (TBA^+) cations play the role of charge-compensating ions but we have proposed that they might also act as structure-directing agents.[23a] These bulky ions occupy the voids delimited by the coordination networks so that none of these structures exhibit accessible porosity. Attempts to exchange these ligands by post-synthetic treatments[29] have also failed. We thus thought to investigate new synthetic methods for replacing TBA^+ cations by cationic coordination complexes,

namely $[M(bpy)_3]^{2+}$ (M = Co, Ru; bpy = 2,2'-bipyridine) complexes (Figure 1b). This study might give new insights into: i) whether ε-Keggin based coordination polymers could form in the absence of TBA^+ counter-ions, ii) whether additional electro(photo)chemical properties into POMOFs could be obtained by introducing the redox non-innocent cations $[M(bpy)_3]^{2+}$ complexes.[30] In addition, we have also attempted to replace the TBA^+ cations with PPh_4^+ counter-ions which have approximately the same size and charge (Figure 1b). We thus report here the synthesis and characterization of four novel hybrid compounds with ε-Keggin POMs connected to di- or tri-carboxylate linkers (Figure 1c) and $[M(bpy)_3]^{2+}$ (M = Co, Ru) or PPh_4^+ counter-ions. The electrochemical activity of these materials for HER is also described.

EXPERIMENTAL SECTION

Synthesis and Characterizations: H_3BTB, $[Co(bpy)_3]Cl_2 \cdot 6H_2O$ and $[Ru(bpy)_3]Cl_2 \cdot 6H_2O$ were synthesized according to reported procedures.[31] All other reagents were purchased from commercial sources and used as received. Molybdenum powder 1-5 μm with purity >99.9% was used for the synthesis. Hydrothermal syntheses were carried out in 23 mL polytetrafluoroethylene lined stainless steel containers under autogenous pressure. All reactants were briefly stirred before heating. The mixture was heated to 200 °C over a period of 1 h, kept at 200 °C for 70 h and cooled down to room temperature over a period of 80 h. The pH mixture was measured before (pH_i) and after the reaction (pH_f). The product was isolated by filtration after sonication which allowed removing a brown powder always present after the reaction and washed with ethanol. The crystalline homogeneity of the compounds was checked by comparison of the experimental X-ray powder pattern with the powder pattern calculated from the structure solved from single-crystal X-ray diffraction data (Figures SI1-SI2). In Figure SI1, the powder pattern of the POMOFs with BTB linkers was compared to the powder pattern calculated from the structure recently called NENU-500.[23c]

Preparation of $(TBA)_4[PMo^{V}_8Mo^{VI}_4O_{37}(OH)_3Zn_4](C_{27}H_{15}O_6)_{4/3}\cdot 1.5C_{27}H_{18}O_6\cdot 8H_2O$ (**ε(BTB)$_{4/3}$**): A mixture of $(NH_4)_6Mo_7O_{24}\cdot 4H_2O$ (0.618 g, 0.50 mmol), metallic Mo (0.060 g, 0.62 mmol), H_3PO_3 (0.060 g, 0.75 mmol), $Zn(CH_3COO)_2\cdot 2H_2O$ (0.219 g, 1 mmol), H_3BTB (0.400 g, 0.91 mmol), tetrabutylammonium hydroxide 40 w.t. % solution in water (200 µL, 0.30 mmol) and H_2O (10 mL) was stirred and the pH was adjusted to 6 with 4 M HCl (pH_f = 5.7). Dark red diplohedral crystals suitable for X-ray diffraction study were collected after filtration (0.108 g, 9.8 % based on Zn). Anal. calc. (found) for $C_{140.5}H_{210}Mo_{12}N_4O_{65}PZn_4$ (M. W. = 4439.0 g mol^{-1}): C 38.01 (38.75), H 4.77 (4.63), Mo 25.93 (24.91), N 1.26 (1.36), Zn 5.89 (6.19). IR (ν/cm^{-1}): 2953 (m), 2926 (m), 2867 (m), 1698 (w), 1594 (m), 1548 (w), 1466 (w), 1375 (s), 1269 (w), 1176 (w), 1099 (w), 964 (sh), 922 (s), 855 (w), 816 (s),781 (s), 700 (m), 673 (sh), 587 (s), 484 (m).

Preparation of $(TBA)_2[Co(C_{10}H_8N_2)_3][PMo^{V}_8Mo^{VI}_4O_{37}(OH)_3Zn_4](C_{27}H_{15}O_6)_{4/3}\cdot 1.5$ $C_{27}H_{18}O_6\cdot 24H_2O$ (**Co-ε(BTB)$_{4/3}$**): A mixture of $(NH_4)_6Mo_7O_{24}\cdot 4H_2O$ (0.618 g, 0.50 mmol), metallic Mo (0.060 g, 0.62 mmol), H_3PO_3 (0.060 g, 0.75 mmol), $Zn(CH_3COO)_2\cdot 2H_2O$ (0.219 g, 1 mmol), H_3BTB (0.400 g, 0.91 mmol), tetrabutylammonium hydroxide 40 w.t. % solution in water (200 µL, 0.30 mmol), $[Co(bpy)_3]Cl_2\cdot 6H_2O$ (0.120 g, 0.17 mmol) and H_2O (10 mL) was stirred and the pH was adjusted to 6 with 4 M HCl (pH_f = 6.1). Dark red diplohedral crystals were collected after filtration and sonication in DMSO (to remove non reacted H_3BTB) and ethanol (0.242 g, 20 % based on Zn). Anal. calc. (found) for $C_{138.5}H_{175}CoMo_{12}N_8O_{72}PZn_4$ (M. W. = 4769.8 g mol^{-1}): C 34.84 (33.86), H 4.10 (3.47), N 2.35 (2.80), Mo 24.17 (24.91), Zn 5.49 (6.19). IR (ν/cm^{-1}): 2958 (w), 2938 (w), 2871 (w), 1594 (m), 1551 (w), 1472 (w), 1441 (m), 1375 (s), 1314 (w), 1248 (w), 1176 (w), 1154 (w), 1104 (w), 1059 (w), 1016 (w), 992 (w), 959 (sh), 934 (s), 920 (s), 852 (w), 813 (m), 779 (s), 762 (s), 735 (sh), 702 (m), 673 (m), 651 (m), 630 (sh), 585 (s), 550 (m), 483 (m).

Preparation of $[Co(C_{10}H_8N_2)_3][PMo^{V}_8Mo^{VI}_4O_{37}(OH)_3Zn_4](C_9H_3O_6)Co(C_{10}H_8N_2)_2(H_2O)\cdot 16H_2O$ (**Co-ε(trim)(bpy)$_2$**): A mixture of $Na_2MoO_4\cdot 2H_2O$ (0.844 g, 3.50 mmol), metallic Mo (0.060 g, 0.62 mmol), H_3PO_3 (0.060 g, 0.75 mmol), $Zn(CH_3COO)_2\cdot 2H_2O$ (0.219 g, 1 mmol), 1,3,5-benzenetricarboxylic acid (0.210 g, 1 mmol), $[Co(bpy)_3]Cl_2\cdot 6H_2O$ (0.300 g, 0.42 mmol), tetrabutylammonium hydroxide 40 w.t. % solution in water (100 μL, 0.15 mmol) and H_2O (10 mL) was stirred and the pH was adjusted to 5 with 4 M HCl (pH_f = 4.8). Black crystals were collected after filtration and sonication in ethanol (0.160 g, 17 % based on Zn). Anal. calc. (found) for $C_{79}H_{95}Co_2Mo_{12}N_{14}O_{63}PZn_4$ (M. W. = 3810.3 g mol^{-1}): C 24.90 (24.77), H 2.51 (2.16), Co 3.09 (2.86), Mo 30.21 (32.51), N 5.15 (5.04), Zn 6.86 (5.72). IR (ν/cm^{-1}): 1597 (m), 1565 (w), 1471 (w), 1440 (m), 1355 (w), 1314 (w), 1156 (w), 1102 (w), 1059 (w), 1021 (w), 930 (s), 751 (s), 734 (sh), 650 (w), 583 (m), 513 (m), 474 (m), 400 (w).

Preparation of $[Ru(C_{10}H_8N_2)_3]_4[PMo^{V}_8Mo^{VI}_4O_{38}(OH)_2Zn_4]_2(C_9H_3O_6)_2\cdot 30H_2O$ (**Ru-ε$_2$(trim)$_2$**): A mixture of $Na_2MoO_4\cdot 2H_2O$ (0.844 g, 3.50 mmol), metallic Mo (0.060 g, 0.62 mmol), H_3PO_3 (0.060 g, 0.75 mmol), $Zn(CH_3COO)_2\cdot 2H_2O$ (0.219 g, 1 mmol), 1,3,5-benzenetricarboxylic acid (0.070 g, 0.33 mmol), $[Ru(bpy)_3]Cl_2\cdot 6H_2O$ (0.120 g, 0.16 mmol) and H_2O (10 mL) was stirred and the pH was adjusted to 5 with 4 M HCl (pH_f = 5.4). Black crystals were collected after filtration and sonication in ethanol (0.140 g, 15 % based on Zn). Anal. calc. (found) for $C_{138}H_{166}Mo_{24}N_{24}P_2O_{122}Ru_4Zn_8$ (M. W. = 7405.19 g mol^{-1}): C 22.38 (21.41), H 2.26 (1.77), N 4.54 (4.29), Mo 31.10 (31.47), Ru 5.46 (4.87), Zn 7.06 (8.18). IR (ν/cm^{-1}): 1618 (m), 1565 (w), 1462 (w), 1444 (w), 1422 (w), 1345 (m), 1312(sh), 1269 (w), 1243 (w), 1160 (w), 1123 (w), 1004 (w), 992 (w), 965 (m), 923 (s), 811 (m), 778 (sh), 758 (s), 728 sh), 704 (m), 591 (m), 539 (m), 484 (m).

Preparation of $[P(C_6H_5)_4]_6[PMo^{V}_8Mo^{VI}_4O_{37}(OH)_3Zn_4]_2(C_9H_3O_6)_2\cdot 18H_2O$ (**PPh$_4$-ε$_2$(trim)$_2$**): A mixture of $Na_2MoO_4\cdot 2H_2O$ (0.844 g, 3.50 mmol), metallic Mo (0.060 g, 0.62 mmol), H_3PO_3

(0.060 g, 0.75 mmol), $Zn(CH_3COO)_2 \cdot 2H_2O$ (0.219 g, 1 mmol), 1,3,5-benzenetricarboxylic acid (0.210 g, 1 mmol), PPh_4Cl (0.061 g, 0.16 mmol) and H_2O (10 mL) was stirred and the pH was adjusted to 5.5 with 4 M HCl (pH_f = 4.8). Black crystals were isolated with tweezers in poor yield (~ 0.040 g) after filtration and sonication in ethanol. Anal. calc. (found) for $C_{162}H_{168}Mo_{24}O_{110}P_8Zn_8$ (M. W. = 6948.5 g mol^{-1}): C 28.00 (28.67), H 2.43 (2.36). Metal composition was checked by EDX analysis. IR (ν/cm^{-1}): 1649 (w), 1617 (w), 1565 (w), 1482 (w), 1436 (m), 1399 (m), 1298 (w), 1188 (w), 1105 (m), 995 w), 980 (sh), 966 (m), 940 (s), 923 (s), 811 (m), 775 (s), 749 (m), 718 (m), 685 (s), 614 (w), 587 (s), 521 (s).

Preparation of $[Ru(C_{10}H_8N_2)_3]_3[PMo^{V}_8Mo^{VI}_4O_{37}(OH)_3Zn_4Cl]_2(C_{14}H_8O_4)_2 \cdot 24H_2O$ (**Ru-ε$_2$(biphen)$_2$**): A mixture of $(NH_4)_6Mo_7O_{24} \cdot 4H_2O$ (0.618 g, 0.50 mmol), metallic Mo (0.060 g, 0.62 mmol), H_3PO_3 (0.060 g, 0.75 mmol), $Zn(CH_3COO)_2 \cdot 12H_2O$ (0.219 g, 1 mmol), biphenyldicarboxylic acid (0.242 g, 1 mmol), $[Ru(bpy)_3]Cl_2 \cdot 6H_2O$ (0.092 g, 0.12 mmol) and H_2O (8 mL) was stirred and the pH was adjusted to 5 with 4 M HCl (pH_f = 4.9). Black crystals were collected after filtration and sonication in ethanol (0.160 g, 19 % based on Zn). Anal. calc. (found) for $C_{118}H_{162}Cl_2Mo_{24}N_{18}O_{122}P_2Ru_3Zn_8$ (M. W. = 7046.7 g mol^{-1}): C 20.11 (20.76), H 2.32 (1.81), N 3.58 (3.42), Cl 1.01 (1.22), Mo 32.68 (32.01), Ru 4.30 (3.84), Zn 7.42 (7.62). IR (ν/cm^{-1}): 1602 (w), 1584 (w), 1541 (w), 1462 (w), 1445 (w), 1422 (w), 1371 (m), 1312 (w), 11270 (w), 1243 (w), 1123 (w), 973 (m), 923 (s), 813 (m), 758 (s), 107 (m), 684 (w), 587 (m), 539 (m), 523 (m), 483 (m), 439 (w).

Crystal Structure Determination. Single crystal X-ray diffraction data collections were carried out by using a Siemens SMART three circle (**Co-ε(trim)(bpy)$_2$**), a Bruker Nonius X8 APEX 2 (**PPh$_4$-ε$_2$(trim)$_2$**) and a Bruker AXS BV (**Ru-ε$_2$(trim)$_2$**, **Ru-ε$_2$(biphen)$_2$**) diffractometer, each equipped with a CCD bidimensional detector using the monochromatised wavelength λ(Mo Kα) = 0.71073 Å. Absorption corrections were based on multiple and symmetry-equivalent reflections in the data set using the SADABS program[32] based on the

method of Blessing.[33] The structures were solved by direct methods and refined by full-matrix least-squares using the SHELX-TL package.[34] Among the three PPh_4^+ cations, one cation could not be located properly in the structure of **PPh_4-ε_2(trim)$_2$** due to severe disorder and the data set was corrected with the program SQUEEZE,[35] a part of the PLATON package of crystallographic software used to calculate the solvent or counter-ion disorder area and to remove its contribution to the overall intensity data. Crystallographic data are given in Table 1 and the complete data can be found in the cif file as Supporting Information. Selected bond distances and valence bond calculations are given in Figures SI3-SI6. Valence bond calculations confirm the oxidation state of the Mo ions and indicate the presence of protons on bridging oxygen atoms of the POMs.

Powder X-ray diffraction data were obtained on a Brüker D5000 diffractometer using Cu radiation (1.54059 Å). EDX measurements were performed on a JEOL JSM 5800LV apparatus. N_2 adsorption isotherms were obtained at 77 K using a BELsorp Mini (Bel, Japan). Prior to the analysis, approximately 50 mg of sample were evacuated at 90 °C under primary vacuum overnight.

Table 1. Crystallographic data for **Co-ε(trim)(bpy)$_2$**, **Ru-ε$_2$(trim)$_2$**, **PPh$_4$-ε$_2$(trim)$_2$** and **Ru-ε$_2$(biphen)$_2$**.

	Co-ε(trim)(bpy)$_2$	**Ru-ε$_2$(trim)$_2$**	**PPh$_4$-ε$_2$(trim)$_2$**	**Ru-ε$_2$(biphen)$_2$**
Empirical formula	$C_{79}H_{59}Co_2Mo_{12}N_{14}O_{51.5}PZn_4$	$C_{69}H_{51}Mo_{12}N_{12}O_{56}PRu_2Zn_4$	$C_{162}H_{168}Mo_{24}O_{110}P_8Zn_8$	$C_{118}H_{88}Cl_2Mo_{24}N_{18}O_{108}P_2Ru_3Zn_8$
Formula weight / g	3589.99	3590.08	6948.23	6747.63
Crystal system	Monoclinic	Orthorhombic	Orthorhombic	Monoclinic
Space group	*P2$_1$/c*	*Pbca*	*Pbca*	*C2/c*
a / Å	14.796(5)	27.0584(5)	27.0083(6)	31.533(1)
b / Å	24.275(8)	27.2448(3)	27.0121(5)	19.972(1)
c /Å	31.846(10)	27.8802(5)	27.8161(6)	34.002(1)
β / °	99.600(8)	90	90	116.103(1)
V / Å^3	11279(6)	20553.3(6)	20293.3(7)	19229.6(13)
Z	4	8	4	4
ρ_{calc} / g cm^{-3}	2.114	2.320	2.274	2.331
μ / mm^{-1}	2.510	2.725	2.517	2.855
Data / Parameters	25870 / 1394	18048 / 1409	29584 / 1117	25103 / 1414
R_{int}	0.1625	0.1092	0.0400	0.0536
GOF	0.887	0.850	1.213	1.206
R (>2σ(I))	R_1[a] = 0.0716	0.0585	0.0285	0.0536
	wR_2[b]= 0.1863	0.1475	0.0787	0.1183

[a] $R_1 = \Sigma||F_o|-|F_c||/\Sigma|F_o|$. [b] $wR_2 = [\Sigma w(F_o^2 - F_c^2)^2/\Sigma w(F_o^2)^2]^{1/2}$

Electrochemical studies. The electrochemical studies were conducted using a potentiostat SP 300 from Bio-Logic (Bio-Logic Science Instruments SAS) and a Rotating Disc Electrode (RDE) (OrigaTrod, from OrigaLys). All electrochemical studies were performed at room temperature in acidic medium (0.1 M H_2SO_4 at pH = 1.0) using ultrapure water produced by a Millipore system (18.2 MΩ cm at 25 ºC). Solutions were deaerated with nitrogen gas (purity 99.998 %) from Air Liquide for at least 15 min before all experiments.

Preparation of the modified electrodes: because of the high insolubility of the POM-based coordination polymers in common solvents, the electrochemical behaviour of these materials was studied in solid state by entrapping them in a carbon paste electrode. Bulk POMOF-carbon mixtures were prepared in a 1 : 2 weight ratio 5 mg of POM-based polymer and 10 mg of carbon black (Vulcan-XC72R; Cabot Corp.) by hand agate mortar grinding to achieve an uniform mixture. A suspension of 1 mg of a POMOF-carbon mixture (hybrid catalyst) in 50 µL of ultrapure water was then prepared prior to all experiments.

For the Cyclic Voltammetry (CV) and the Linear Sweep Voltammetry (LSV), the modified electrodes were prepared by deposition of 30 µL of the hybrid catalyst on a 3 mm diameter glassy carbon disc electrode (GC) carefully polished on wet polishing cloth using a 1 µm diamond suspension and a 0.05 µm alumina slurry (POMOF-carbon/GC). The deposits were dried under a small flow of argon and protected by deposition of Nafion® (30 µL of Nafion® 5 % in ethanol). The Nafion® layer was then left to dry under a small flow of argon to reach the final modified electrode (Nafion/POMOF-carbon/GC). The modified RDE electrodes used in LSV and electrolysis experiments were prepared using the same method by deposition of 50 µL of suspension on a 3 mm diameter GC and 50 µL of Nafion® 5 % in ethanol (Nafion/POMOF-carbon/GC).

CV (static electrode) and LSV (rotation speed 1000- 2000 rpm) experiments were performed in a conventional three-electrode single-compartment cell. A Pt wire was used as the counter electrode and a saturated Ag/AgCl/KCl electrode (separated from the solution by a salt bridge) as the reference electrode. LSV measurements were conducted after 200 cycles of activation (stable LSV) in the range of 0.2 to -1 V (*vs.* Ag/AgCl) at 100 mV s^{-1} and 2000 rpm to stabilize the current.

Controlled potential electrolysis (CPE) experiments were carried out at room temperature in a gas-tight two-compartment electrochemical cell. The cathodic compartment was separated

from the anodic compartment via a glass frit of fine porosity. The counter electrode was a platinum wire and the reference electrode was a saturated Ag/AgCl/KCl electrode separated by a salt bridge. The activated Nafion/POMOF-carbon/GC electrodes were used as working electrodes. The solutions were purged with N_2 gas for at least 15 min before electrolysis and were constantly stirred. Hydrogen bubbles formed on the surface of the working electrode and attached to it were removed by a brief rotation at 2000 rpm. Production of H_2 in the headspace gas (22 mL) was measured by gas chromatography analysis (Shimadzu GC-2014) with a thermal conductivity detector.

Hybrid catalysts characterization after electrochemical activation.

In order to verify any potential contamination of the POMOF-carbon mixture from the Pt counter electrode, different analyses were performed. The amount of Pt deposited onto the POMOF-carbon/GC electrodes was measured by inductively coupled plasma mass spectrometer (ICP-MS). The samples (0.010 g of POMOF-carbon) after LSV were recuperated by rinsing the electrode surface with ethanol, digested by HCl : HNO_3 = 3 : 1 solution and left to react for 48 h. Note that different batches were accumulated to analyse a larger mass of sample. Then, the sample mixture was diluted to 25 mL of doubly-distilled water, filtered through a 0.45 µm PTFE filter and analysed by a quadrupole based ICP-MS (Thermo Elemental., VG PQ Excell™). EDX analyses were also performed in order to detect the presence of Pt in the POMOF-carbon mixture after electrolysis.

RESULTS AND DISCUSSION

Synthesis and Characterizations. **Co-ε(BTB)$_{4/3}$** and **ε(BTB)$_{4/3}$** are obtained as black diplohedral crystals (Figure SI7) from the hydrothermal reaction of ammonium heptamolybdate, metallic Mo as reducing agent, Zn^{II} ions, H_3BTB and TBA(OH). Compared to previously reported εZn-based POMOF materials,[22b,23,24,25] the synthesis has been

performed at higher pH (6). $[Co(bpy)_3]Cl_2$ was added as a substrate for the synthesis of **Co-ε(BTB)$_{4/3}$**. The presence of TBA(OH) was nevertheless required to get crystals and it was thus impossible to replace all the TBA^+ cations in **ε(BTB)$_{4/3}$**. A compound close to **ε(BTB)$_{4/3}$**, called NENU-500, was recently reported.[23c] Its synthesis, as well as its chemical formula, are slightly different from those of **ε(BTB)$_{4/3}$**. Elemental analysis of **ε(BTB)$_{4/3}$** showed a large excess of C which could only be explained by the presence of extra neutral linkers within the structure. This was confirmed by the presence of a C=O vibration at $\nu_{C=O}$ =1698 cm^{-1} in the IR spectrum (Figure SI8a) characteristic of carboxyl COOH groups. These results, together with TGA curves (Figure SI9), allow to propose the $(TBA)_4[PMo^{V}_8Mo^{VI}_4O_{37}(OH)_3Zn_4](BTB)_{4/3}\cdot 1.5H_3BTB\cdot 8H_2O$ detailed formula for **ε(BTB)$_{4/3}$**. The latter differs from that of NENU-500, $(TBA)_3[PMo^{V}_8Mo^{VI}_4O_{36}(OH)_4Zn_4](BTB)_{4/3}\cdot x$Guest.[23c] The absence of visible white impurities, as well as the absence of extra peaks in the powder diffraction pattern (Figure SI1), suggests that the extra neutral H_3BTB molecules do not co-crystallize with the POMOF but are rather encapsulated within the pores, as commonly observed during MOF synthesis. Attempts to remove the trapped H_3BTB by washing the compound in hot DMF using a Soxhlet apparatus have failed.

Co-ε(BTB)$_{4/3}$ and **ε(BTB)$_{4/3}$** differ by the presence of one $[Co(bpy)_3]^{2+}$ which replaces two TBA^+ cations. In the IR spectra of **Co-ε(BTB)$_{4/3}$** , the presence of εZn POMs with Mo-O vibrations at around ν_{Mo-O} = 920 and 780 cm^{-1}, carboxylate linkers with C-O vibrations at ν_{C-O} = 1548, 1594 and 1698 cm^{-1} and TBA^+ cations with C-H vibrations at around ν_{C-H} =2900 cm^{-1} and at δ_{C-H} =1466 cm^{-1} can be identified (Figure SI8a). However, the intensity of the bands attributed to TBA^+ cations is lower in **Co-ε(BTB)$_{4/3}$** compared to **ε(BTB)$_{4/3}$** and new vibrations are assigned to the bpy ligands, thus confirming the partial substitution of TBA^+ cations.

Black crystals of **Co-ε(trim)(bpy)$_2$** are isolated at pH 5.0, with trimesic acid in place of H_3BTB. Under hydrothermal conditions, some of the $[Co(bpy)_3]^{2+}$ complexes lose one bpy ligand which then chelates Zn^{II} ions of the ε-Keggin unit.

Ru-ε$_2$(trim)$_2$ and **Ru-ε$_2$(biphen)$_2$** are isolated under similar conditions with $[Ru(bpy)_3]Cl_2$ as the reactant. The Ru complex being more stable than its Co analogue, no decomposition could be observed. These phases are not isostructural with previously reported coordination polymers with TBA^+ counter-ions. However, it was possible to synthesize **PPh$_4$-ε$_2$(trim)$_2$** which is isostructural to **Ru-ε$_2$(trim)$_2$**, thus allowing us to explore the influence of the counter-ions on the electrochemical properties. The IR spectra of **Ru-ε$_2$(trim)$_2$** and **PPh$_4$-ε$_2$(trim)$_2$** clearly show the presence of $[Ru(bpy)_3]^{2+}$ and PPh_4^+ counter-ions respectively (Figure SI8b).

Structures. ε(BTB)$_{4/3}$ is isostructural to NENU-500 (Figure SI1a).[23c] Its structure can be briefly described[22c] as a 3D POMOF hybrid network with the monomeric mixed-valent {ε-$PMo^{V}_8Mo^{VI}_4O_{40}Zn_4$} POM (Figure 1a) as the inorganic building unit. Each of the four capping Zn^{II} ions in tetrahedral coordination is bound to three oxygen atoms of the POMs and to an oxygen atom of a BTB acting as a monodentate linker (Figure 2a). The ligands are far from being planar, as commonly observed for structures with BTB.[36] The connection of the POMs by the tritopic linkers generates two interpenetrated 3D networks (Figure 2b). This network possesses a **ctn** topology (Figure SI10), which is one of the few predicted (3,4) periodic nets resulting from the linking of tetrahedral units with triangular linkers.[23a]

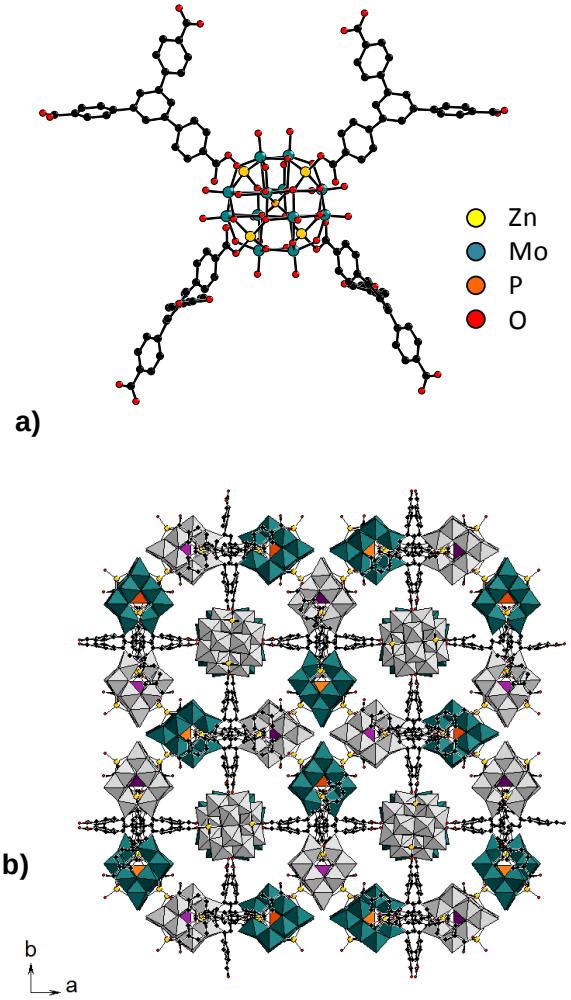

Figure 2. a) The building unit common in **ε(BTB)$_{4/3}$** and **Co-ε(BTB)$_{4/3}$**; b) view along the *c* axis of two interpenetrated 3D networks built from the connection of the building units; the MoO_6 octahedra and PO_4 tetrahedra of the εZn POM units of the first network are blue and orange respectively while those of the second network are grey and purple, respectively.

This structure is thus different from that observed with the trim linker and also from that recently obtained with BTB linkers which contains dimeric $(\varepsilon Zn)_2$ units.[37] Powder X-ray diffraction experiments indicate that **Co-ε(BTB)$_{4/3}$** and **ε(BTB)$_{4/3}$** are isostructural (Figure SI1).

The structure of **Co-ε(trim)(bpy)$_2$** is unprecedented. In this compound, the building unit is the molecular εZn POM (Figure 3a) with two of the Zn^{II} ions chelated by one bpy ligand, the other two Zn^{II} ions being connected to one oxygen atom of a trim linker.

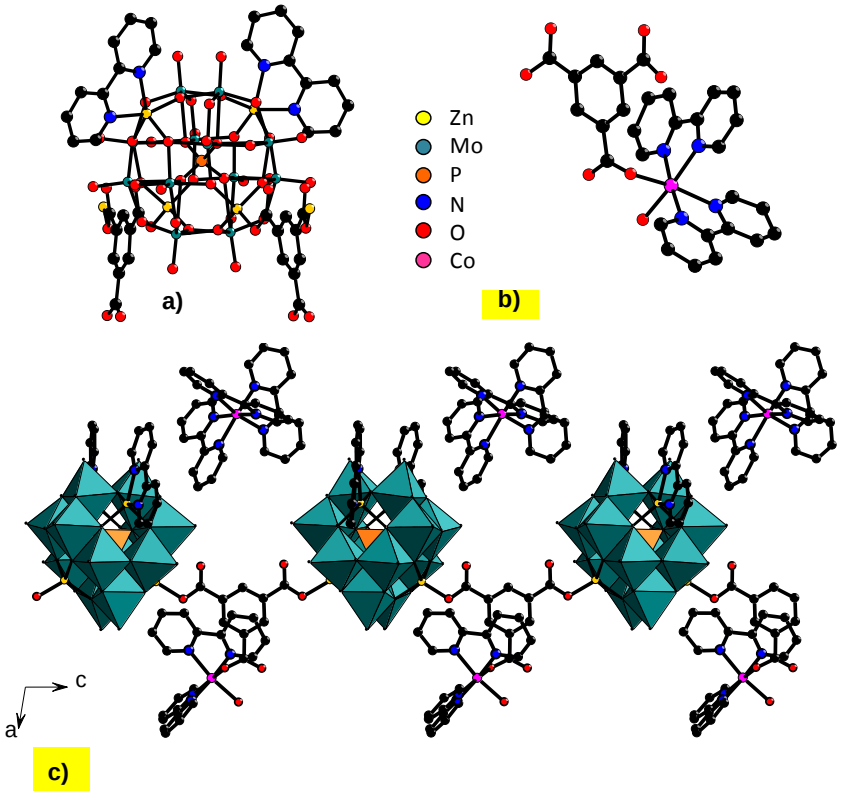

Figure 3. a) The POM building unit in **Co-ε(trim)(bpy)$_2$**; b) the cobalt complex attached to the chain; c) view along the *b* axis of the chain built from the connection of the building units and the non-coordinated $[Co(bpy)_3]^{2+}$ complexes.

These bpy molecules arising from the decomposition of some of the $[Co(bpy)_3]^{2+}$ complexes act as blocking ligands. The connection of the εZn POMs via two carboxylate groups of trim linkers thus leads to a 1D chain (Figure 3b). The third carboxylate group of these trim ligands is bound to the Co^{II} ion of the $[Co(bpy)_2]^{2+}$ fragments where Co also completes its coordination sphere with one water molecule (Figure 3c). Intact $[Co(bpy)_3]^{2+}$ complexes are located in the voids between the chains.

In **Ru-ε$_2$(trim)$_2$** the molecular unit is the dimeric $(\varepsilon Zn)_2$ POM which results from the condensation of two Keggin units via two Zn-O bonds (Figure 4a). The six remaining Zn ions are coordinated to a monodentate carboxylate group of a trim linker. The resulting coordination network is 3D and is different from that in $(TBA)_3[PMo_{12}O_{37}(OH)_3Zn_4][C_6H_3(COO)_3]$ (**TBA-ε$_2$(trim)$_2$**),[23a] even though both structures

incorporate dimeric units. In contrast, the use of PPh_4^+ cations leads to the formation of **PPh_4-ε_2(trim)$_2$** isostructural to **Ru-ε_2(trim)$_2$**.

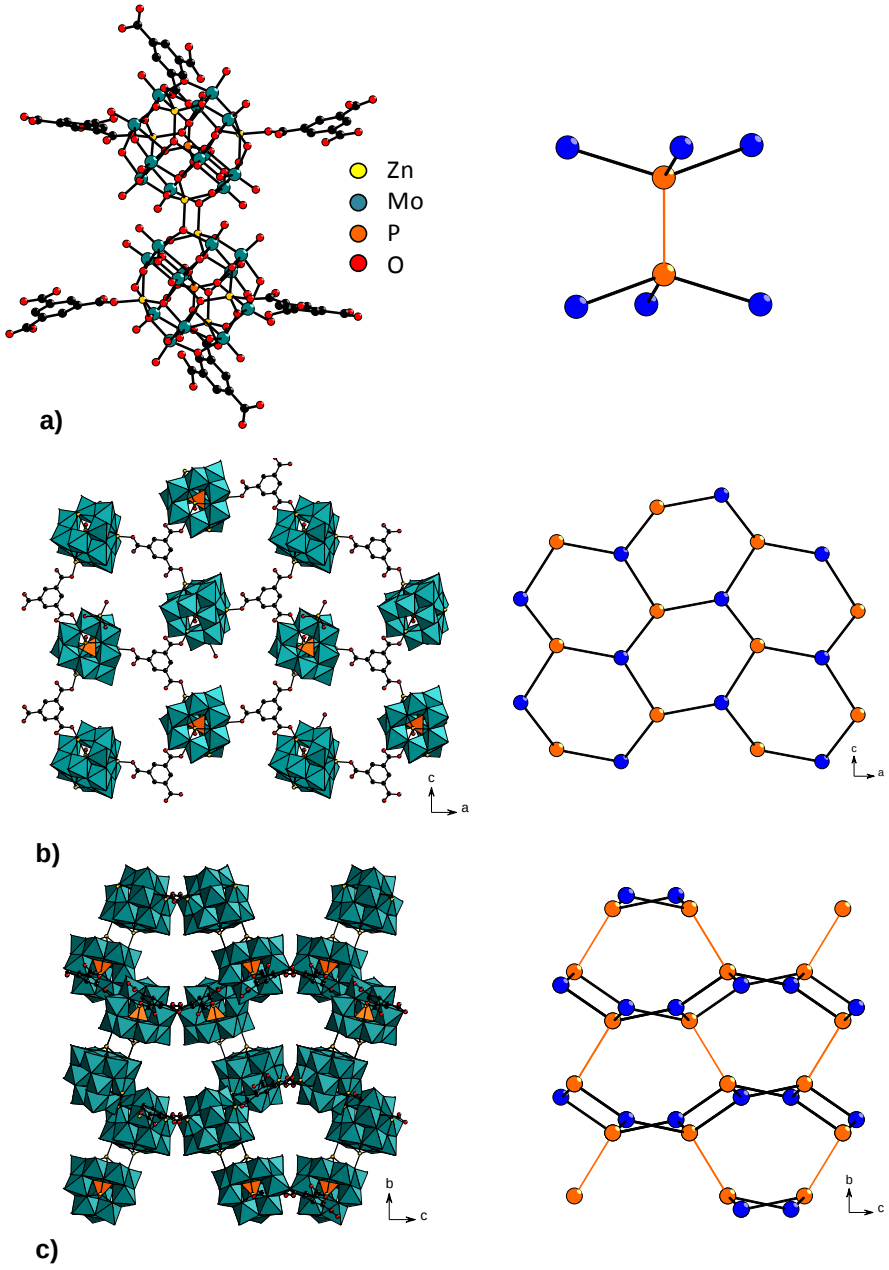

Figure 4. a) The dimeric building unit common in **Ru-ε_2(trim)$_2$** and **PPh_4-ε_2(trim)$_2$**; on the right, the POM is schematized by its centroid, which coincides with the central P atom (orange sphere) and the ligand by its center of mass (blue sphere); b) view of a plane formed by the connection of one εZn moiety of the dimeric $(\varepsilon Zn)_2$ units by trim linkers; on the right the same colour code is used for a simpler representation of the network; c) view of the crystal structure along the *a* axis obtained by the connections of the planes; on the right the same colour code is used for a simpler representation of the network.

This can be explained by the orientations of the trim linkers which are almost parallel in **TBA-ε$_2$(trim)$_2$** while they adopt two different orientations in **Ru-ε$_2$(trim)$_2$** and **PPh$_4$-ε$_2$(trim)$_2$** (Figure SI11). One εZn moiety of a dimeric unit is connected to three neighbouring εZn POMs via trim linkers, forming a distorted honeycomb structure (Figure 4b). The connections of POMs within the dimeric $(\varepsilon Zn)_2$ units allows the connection of the planes into a 3D network (Figure 4c). The negative charge of the network is compensated by 3 protons for one POM unit, located on the bridging oxygen atoms (Figure SI5), by 3 PPh_4^+ cations in **PPh$_4$-ε$_2$(trim)$_2$** and by 2 protons and 2 $[Ru(bpy)_3]^{2+}$ complexes in **Ru-ε$_2$(trim)$_2$**. The positions of these counter-ions are shown in Figure SI12. No π-π interaction has been identified in any of these structures.

In **Ru-ε$_2$(biphen)$_2$**, dimeric $(\varepsilon Zn)_2$ POMs make bonds with monodentate biphen carboxylates (Figure 5a). However, in contrast with **Ru**- and **PPh$_4$-ε$_2$(trim)$_2$**, this is true for only four Zn(II) ions out of six, the other two bearing terminal chloride ions coming from the $[Ru(bpy)_3]Cl_2$ precursor. Consequently, the structure is only 2D; the planes stack along the *a* axis (Figures 5b and c). Three $[Ru(bpy)_3]^{2+}$ complexes, one of which is disordered over two positions, occupy the voids delimited by the connection of the POMs and the biphen linkers so that the structure is very compact. It should be noted that the structure of this compound is different from that of **ε$_2$(biphen)$_3$**, the related compound previously reported with TBA^+ counter-ions instead of Ru complexes.[23b]

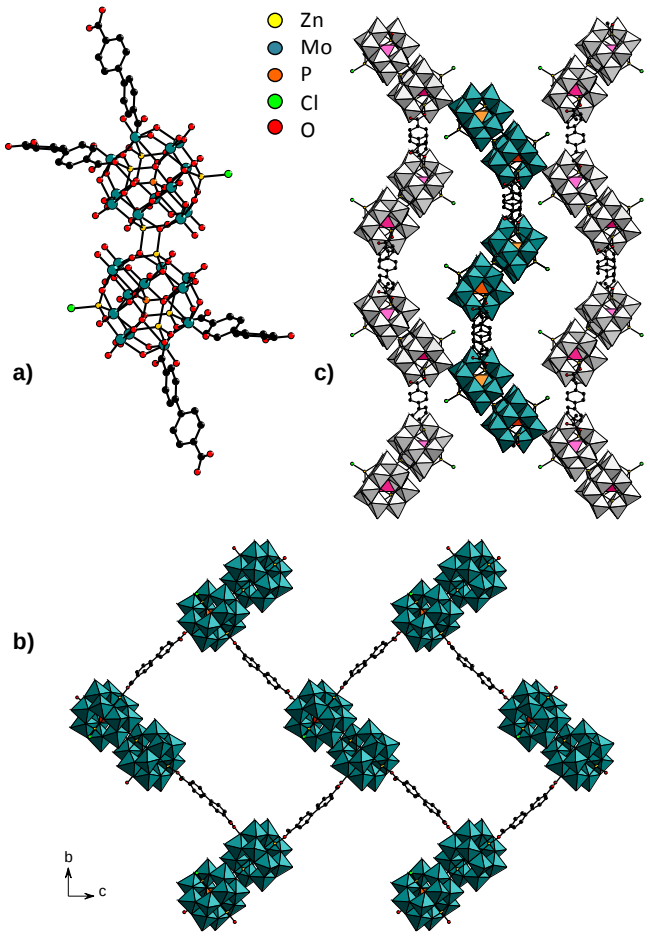

Figure 5. a) The dimeric building unit in **Ru-ε$_2$(biphen)$_2$**; b) view along the *a* axis of a plane built from the connection of the (εZn)$_2$ units; c) view of the stacking of three consecutive planes; the MoO_6 octahedra and PO_4 tetrahedra of the (εZn)$_2$ POM units of the first plane are blue and orange respectively while those of the two adjacent planes are grey and purple, respectively.

Electrochemical characterization. The electrochemical behaviour of these POMOFs was studied in the solid state by entrapping them in a carbon paste electrode as described in the experimental section. A suspension of a POMOF-carbon mixture in water was deposited on a previously polished GC (glassy carbon) electrode and was covered by a layer of Nafion®. Cyclic voltammograms (CVs) were performed in 0.1 M H_2SO_4 aqueous solution at potentials ranging from −0.25 to +0.55 V (vs. Ag/AgCl). In the following, potentials are related to the silver chloride electrode (E= 0.2 V vs NHE and – 0.2 V vs ferrocene). We have checked the stability of the compounds in the electrolyte solutions. The absence of any significant change of the IR spectrum and of the powder X-ray diffraction pattern of **Ru-ε$_2$(biphen)$_2$** (taken as a

representative example of the family) stirred for 20 h in 0.1 M H_2SO_4 confirmed that this POMOF did not decompose in this aqueous media (Figure SI13).

The CVs displayed the three well-defined characteristic waves **I**, **II**, **III** and a fourth anodic wave in some cases not well-defined (**IV**) (Figure 6 and Figures SI14-18). These bielectronic waves (**I**, **II** and **III**) are assigned to three different Mo^{VI}/Mo^{V} redox processes of the Mo centers of the polyoxomolybdate ε-Keggin.[22a,22c,23,24,38] Upon increasing the pH, a shift towards more cathodic potentials was observed for all the redox processes together with a decrease in the peak current intensity. This confirms the role of protons accompanying the reduction of the POM-based polymer by incorporating positive charges to the electrode surface to maintain neutrality [23b,37] according to the following equation:

$$POMOF + 2e^- + 2H^+ \leftrightarrows H_2POMOF$$

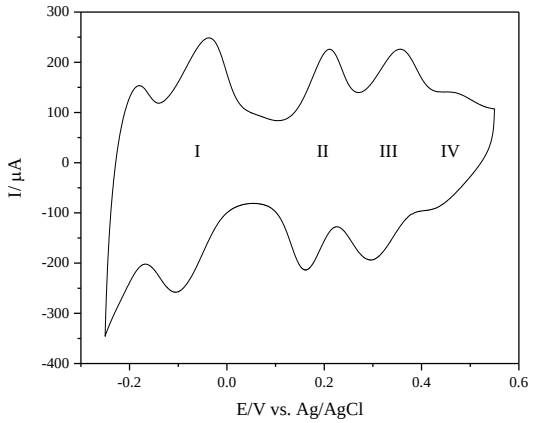

Figure 6. Cyclic voltammogram of **Co-ε(trim)(bpy)$_2$** in 0.1 M H_2SO_4 (pH = 1.0) at a scan rate of 50 mV s^{-1}, third scan.

Half-wave potential $E_{1/2} = (E_{pa} + E_{pc})/2$ and potential peak separation ($\Delta E = |E_{pa} - E_{pc}|$) values regarding main waves **I**, **II** and **III** are reported in Table SI1 for the six compounds in 0.1 M H_2SO_4 (pH = 1.0). The $E_{1/2}$ values are independent of the scan rate and the current intensities ratio (I_{pa}/I_{pc}) is ~ 1 which suggests a highly reversible process.

Figure SI18 displays CVs for **ε(BTB)$_{4/3}$** as a function of the scan rate. The linear dependence of the peak current intensity with respect to the scan rate is consistent with a surface-controlled redox process.[23] Similarly, the CV recorded under a high rotation rate gives the same profile as the static CV, which confirms that the process is not governed by diffusion of the species in solution but rather due to an adsorbed species (Figure SI20).

The $E_{1/2}$(II) potentials of the wave **II** are the same for all materials and seem unaffected by the structural or counter ion variations. On the contrary, $E_{1/2}$(I) and $E_{1/2}$(III) potentials of the waves **I** and **III** vary slightly depending on these parameters. Indeed, the main peak potentials for the redox couple **I** was found to be $E_{1/2}$(I) = -0.07 V *vs*. Ag/AgCl for **Co-ε(trim)(bpy)$_2$**, **ε(BTB)$_{4/3}$** and **Co-ε(BTB)$_{4/3}$** and $E_{1/2}$(I) ≈ -0.09 V *vs*. Ag/AgCl for **Ru-ε$_2$(trim)$_2$**, **PPh$_4$-ε$_2$(trim)$_2$** and **Ru-ε$_2$(biphen)$_2$**. The frameworks with dimeric (εZn)$_2$ POM units tend to have lower $E_{1/2}$(I) values than those with monomeric POM units. The same trend was observed for $E_{1/2}$(III). Moreover, the counter ions have a slight influence on the $E_{1/2}$(III) potential of the wave **III** as can be seen from comparison within the **ε$_2$(trim)$_2$** type frameworks ($E_{1/2}$(III) = 0.32 V for **Ru-ε$_2$(trim)$_2$** and $E_{1/2}$(III) = 0.30 V for **PPh$_4$-ε$_2$(trim)$_2$**).

Electrocatalytic response of the hybrid materials. The HER catalytic activities of the POM-based coordination polymers were evaluated by LSV reaching negative potentials down to -1 V *vs*. Ag/AgCl. The POMOF-carbon mixture was deposited on a GC electrode as described in the experimental section. These experiments were conducted in 0.1 M H_2SO_4 aqueous solutions (pH = 1.0) using a RDE rotating at 2000 rpm. For all compounds, at potentials below -0.6 V *vs*. Ag/AgCl a catalytic wave was observed and assigned to the reduction of protons. After this scan, the characteristic CV observed for these compounds could not be recovered (see Figure SI21). This behaviour has been attributed to a multielectronic irreversible reduction process of Mo species.[23] To reach their maximum HER activities the materials were thus activated by a cycling process (200 cycles) from 0.2 V to -1

V at a scan rate of 100 mV s^{-1} (Figure SI22). During these cycles, the activity gradually increased to reach a maximum onset potential, ranging from -260 mV to -450 mV (Table 2). Thus, the initial POM-based polymers act as precatalysts for the formation of HER active materials, although the mechanism of this activation remains unknown. The formation of platinum nanoparticles on the electrode surface as suggested by Kulesza *et al.*[39] and Zhang *et al.*[40] has not been evidenced. Indeed both EDX and ICP-MS analysis failed at revealing the presence of any Pt (minimum concentration detected ≤ 1 ppb). Figure 7 shows the LSV curves after the activation process of the POMOF materials. Taking into account that a solar light-coupled HER apparatus usually runs at a current density of 10-20 mA cm^{-2},[41] the overpotential for a current of 10 mA cm^{-2} (η_{10}) is chosen as a point of reference to compare the HER activities of the materials (Table 2).

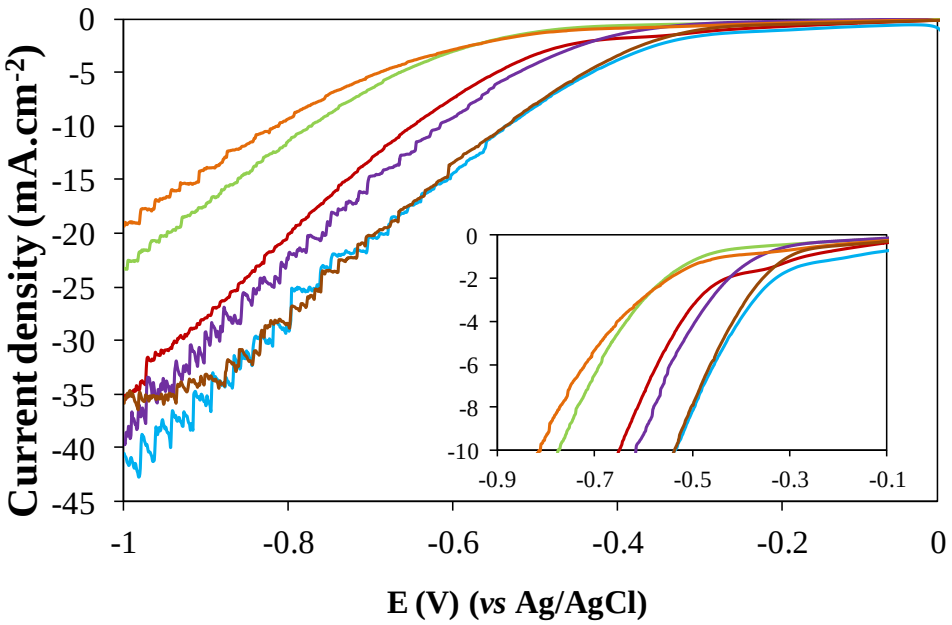

Figure 7. LSV curves after 200 cycles of activation of the POM-based materials in 0.1 M H_2SO_4 (pH = 1.0) at 2000 rpm and at a scan rate of 5 mV s^{-1}. **Co-ε(trim)(bpy)$_2$** (red), **ε(BTB)$_{4/3}$** (green), **Co-ε(BTB)$_{4/3}$** (magenta), **Ru-ε$_2$(trim)$_2$** (orange), **PPh$_4$-ε$_2$(trim)$_2$** (blue) and **Ru-ε$_2$(biphen)$_2$** (brown). Inset: zoom showing the LSV curves with current up to -10 mA cm^{-2}.

Considering the onset potential and overpotential values, three groups of POMOF materials can be distinguished. **Ru-ε$_2$(biphen)$_2$** and **PPh$_4$-ε$_2$(trim)$_2$** have the lowest onset potential

(around -260 mV and 270 mV *vs*. Ag/AgCl, respectively) and the lowest η_{10} value (~ 336 mV), **Ru-ε$_2$(trim)$_2$** has the highest values, and the three other materials, **Co-ε(BTB)$_{4/3}$**, **ε(BTB)$_{4/3}$** and **Co-ε(trim)(bpy)$_2$**, have intermediate values.

Table 2. Comparison of the HER activity and H_2 production of the POM-based coordination polymers.

Catalyst	Dimensionality	POM Building unit	Onset potential/mV	η_{10}/ mV[a]	H_2 evolution rate/nmol min^{-1} [b]	FY_{60} (%)[c]
Co-ε(trim)(bpy)$_2$	1D	εZn	-410	452	140	54
ε(BTB)$_{4/3}$	3D	εZn	-450	576	250	57
Co-ε(BTB)$_{4/3}$	3D	εZn	-310	419	235	52
Ru-ε$_2$(trim)$_2$	3D	(εZn)$_2$	-450	617	110	71
PPh$_4$-ε$_2$(trim)$_2$	3D	(εZn)$_2$	-270	335	670	52
Ru-ε$_2$(biphen)$_2$	2D	(εZn)$_2$	-260	337	510	49

[a] η_{10} is defined as the overpotential measured for a current of 10 mAcm^{-2}. In order to calculate the HER overpotential, platinum electrode is taken as reference material ($E_{Pt/H2} \approx 0.2$ V *vs.* Ag/AgCl). [b] H_2 evolution rate after the five first minutes of electrolysis at -0.6 V *vs.* Ag/AgCl. [c] Faradic yield after 60 min of electrolysis at -0.6 V vs. Ag/AgCl.

Controlled potential electrolysis. To confirm the electrocatalytic HER and examine the durability of these POM-based polymer materials, CPE experiments were conducted at -0.6 V *vs.* Ag/AgCl in 0.1 M H_2SO_4 aqueous solution at pH = 1.0. The first direct observation of the production of hydrogen is the intense formation of bubbles at the surface of the electrode shortly after the beginning of the CPE. H_2 production was measured during CPE experiments by gas chromatography (Figure 8 and Table 2). We observed that the production of H_2 for all catalysts studied here reaches a plateau at around 60 minutes. Faradic yields are calculated after 60 minutes reaction yielding values at around 60 %, which is underestimated, since the charge consumed to reach the active reduced Mo species has not been taken into account.

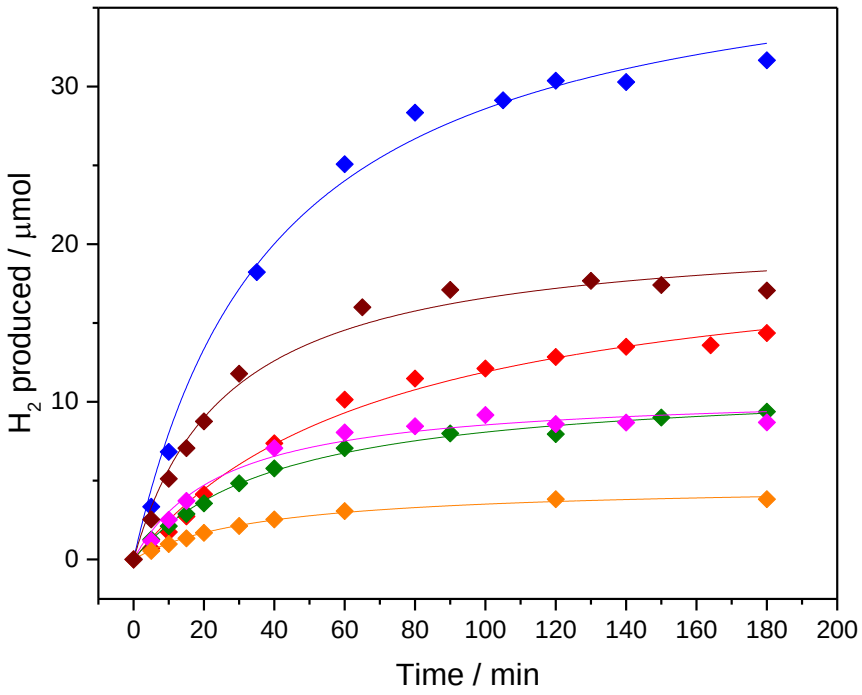

Figure 8. Hydrogen production during the CPE at -0.6 V vs Ag/AgCl in 0.1 M H_2SO_4 (pH = 1.0). **Co-ε(trim)(bpy)$_2$** (red), **ε(BTB)$_{4/3}$** (green), **Co-ε(BTB)$_{4/3}$** (magenta), **Ru-ε$_2$(trim)$_2$** (orange), **PPh$_4$-ε$_2$(trim)$_2$** (blue) and **Ru-ε$_2$(biphen)$_2$** (brown).

Ru-ε$_2$(biphen)$_2$ and **PPh$_4$-ε$_2$(trim)$_2$** which have the lowest η_{10} values have also the highest H_2 evolution rates while **Ru-ε$_2$(trim)$_2$** is the least active compound. A trend on the effect of the cations in POM-based polymers for the HER arises from these results. The presence of big divalent counter ions such as $[M(bpy)_3]^{2+}$ (M = Co or Ru) tends to decrease the catalytic performances of the materials compared to monovalent cations like TBA^+ or PPh_4^+. Indeed, for the isostructural **ε$_2$(trim)$_2$** type frameworks, **PPh$_4$-ε$_2$(trim)$_2$** is far more active than **Ru-ε$_2$(trim)$_2$**. On the contrary, neither the dimensionality of the framework nor the nature of the POM building unit seems to have an effect on the catalytic activity.

CONCLUSION

In conclusion, we have evidenced for the first time that the TBA^+ counter-ions usually present in ε-Keggin-based coordination polymers may be replaced *in situ*, partially or totally, with $[M(bpy)_3]^{2+}$ (M = Ru, Co) or PPh_4^+ counter-ions. In **Co-ε(BTB)$_{4/3}$** half of the TBA^+ cations

were substituted leaving the hybrid structure of the compound unchanged compared to the structure with TBA^+ cations only. By contrast, there are no TBA^+ cations left in the three novel coordination polymers **PPh_4-ε$_2$(trim)$_2$**, **Ru-ε$_2$(trim)$_2$**, and **Ru-ε$_2$(biphen)$_2$** which contain PPh_4^+ cations or $[Ru(bpy)_3]^{2+}$ as counter-cations. Also, their structures are different from their analogues containing TBA^+ counter-ions, showing that the counter-ions have indeed a structure-directing role. Furthermore, it has been possible to isolate the unprecedented 1D coordination polymer **Co-ε(trim)(bpy)$_2$** with two types of Co^{II}-containing complexes, one covalently attached to the 1D chains and the other located in the voids as counter-ions. Finally, these materials act as precatalysts for the hydrogen evolution reaction. Their activity depends strongly on the nature of the counter-ions. **PPh_4-ε$_2$(trim)$_2$** appears as the most efficient compound in terms of onset potential (-270 mV) and hydrogen production. The comparison of its activity with that of the isostructural **Ru-ε$_2$(trim)$_2$** suggests that monocationic counter-ions are more favourable than dicationic ones for the electrocatalytic activity.

ASSOCIATED CONTENT

Supporting Information: Comparison of the experimental X-ray powder patterns and of the powder patterns calculated from the structure solved from single crystal X-ray diffraction, selected bond distances, bond valence sums, infrared spectra, TGA analysis, additional figures of the structure, cyclic voltammograms and linear sweep voltammograms. This material is available free of charge via the Internet at http://pubs.acs.org.

Accession codes: Crystallographic data for new structures reported herein were deposited with the Cambridge Crystallographic Data Centre and allocated the deposition numbers CCDC 1514574-1514577. These data can be obtained free of charge from the Cambridge Crystallographic Data Centre via www.ccdc.cam.ac.uk/data_request/cif.

AUTHOR INFORMATION

Corresponding Authors

*E-mail: maria.gomez@college-de-france.fr, marc.fontecave@college-de-france.fr, anne.dolbecq@uvsq.fr

ACKNOWLEDGMENTS

This work was supported by the Ministère de l'Enseignement Supérieur et de la Recherche, the CNRS, the Université de Versailles Saint Quentin en Yvelines, the Collège de France and a public grant overseen by the French National Research Agency (ANR) as part of the "Investissements d'Avenir" program n°ANR-11-IDEX-0003-02 and CHARMMMAT ANR-11-LABX-0039. We acknowledge support from Fondation de l'Orangerie for individual Philanthropy and its donors. Khaoula Mazouzi and Clotilde Menet are gratefully acknowledged for their participation to the synthesis.

REFERENCES

(1) (a) Batten, S. R.; Champness, N. R.; Chen, X.-M.; Garcia-Martinez, J.; Kitagawa, S.; Öhrström, L.; O'Keeffe, M.; Suh, M. P.; Reedijk, J. *Cryst. Eng. Comm*. **2012**, *14*, 3001. (b) Special issue of *Chem. Soc. Rev.* **2014**, *43*, 5415. (c) Stock, N.; Biswas, S. *Chem. Rev*. **2012**, *112*, 933.

(2) Dolbecq, A.; Mialane, P.; Sécheresse, F.; Keita, B.; Nadjo, L. *Chem. Commun*. **2012**, *48*, 8299.

(3) (a) Miras, H. N.; Yan, J.; Long, D.-L.; Cronin, L. *Chem. Soc. Rev*. **2012**, *41*, 7403. (b) Proust, A.; Matt, B.; Villanneau, R.; Guillemot, G.; Gouzerh, P.; Izzet, G. *Chem. Soc. Rev.* **2012**, *41*, 7605. (c) Sartorel, A.; Bonchio, M.; Campagna, S.; Scandola, F. *Chem. Soc. Rev.*

2013, *42*, 2262. (d) Bassil, B. S.; Kortz, U. *Z. Anorg. Allg. Chem.* **2010**, *636*, 2222. (e) Müller, A.; Gouzerh, P. *Chem. Soc. Rev.* **2012**, *41*, 7431.

(4) (a) Clemente-Juan, J. M.; Coronado, E.; Gaita-Ariño, A. *Chem. Soc. Rev.* **2012**, *41*, 7464. (b) Kögerler, P.; Tsukerblat, B.; Müller, A. *Dalton Trans*. **2010**, *39*, 21. (c) Yin, P.; Li, D.; Liu, T. *Chem. Soc. Rev*. **2012**, *41*, 7368. (d) Dolbecq, A.; Mialane, P.; Keita, B.; Nadjo, L. *J. Mat. Chem*. **2012**, *22*, 24509.

(5) (a) du Peloux, C. ; Dolbecq, A. ; Mialane, P. ; Marrot, J. ; Rivière, E. ; Sécheresse, F. *Angew. Chem. Int. Ed*. **2001**, *40*, 2455. (b) Streb, C.; Ritchie, C.; Long, D.-L.; Kögerler, P.; Cronin, L. *Angew. Chem. Int*. **2007**, *119*, 7723. (c) Ritchie, C.; Streb, C.; Thiel, J.; Mitchell, S. G.; Miras, H. N.; Long, D.-L.; Boyd, T.; Peacock, R. D.; McGlone, T.; Cronin, L. *Angew. Chem. Int. Ed.* **2008**, *47*, 6881. (d) Zhang, Z.; Sadakane, M.; Murayama, T.; Izumi, S.; Yasuda, N.; Sakaguchi, N.; Ueda, W. *Inorg. Chem*. **2014**, *53*, 903.

(6) (a) Du, D.-Y.; Qin, J.-S.; Li, S.-L. ; Su, Z.-M. ; Lan, Y.-Q. *Chem. Soc. Rev*. **2014**, *43*, 4615. (b) He, W. W.; Li, S.-L; Zhang, H.-Y.; Yang, G.-S.; Zhang, S.-R.; Su, Z.-M. ; Lan, Y.-Q. *Coord. Chem. Rev*. **2014**, *279*, 141.

(7) (a) Yao, S.; Yan, J.-H.; Duan, H.; Zhang, Z.-M.; Li, Y.-G.; Han, X.-B.; Shen, J.-Q.; Fu, H.; Wang, E.-B. *Eur. J. Inorg. Chem*. **2013**, 4770. (b) An, H.-Y.; Wang, E.-B.; Xiao, D.-R.; Li, Y.-G.; Su, Z.-M.; Xu, L. *Angew. Chem. Int. Ed*. **2006**, *45*, 904. (c) Liu, C.-M.; Zhang, D.-Q.; Zhu, D.-B. *Cryst. Growth Des*. **2006**, *6*, 524. (d) Martín-Caballero, J.; San José Wéry, A. ; Reinoso, S.; Artetxe, B.; San Felices, L.; El Bakkali, B.; Trautwein, G.; Alcañiz-Monge, J.; Luis Vilas, J.; Gutiérrez-Zorrilla, J. M. *Inorg. Chem*. **2016**, *55*, 4970. (e) Compain, J.-D.; Nakabayashi, K.; Ohkoshi, S.-I. *Inorg. Chem*. **2012**, *51*, 4897.

(8) (a) Lei, C.; Mao, J.-G.; Sun, Y.-Q.; Song, J.-L. *Inorg. Chem*. **2004**, *43*, 1964. (b) Mandic, S.; Heakey, M. R.; Gotthardt, J. M.; Alley, K. G.; Gable, R. W.; Ritchie, C.; Boskovic, C.

Eur. J. Inorg. Chem. **2013**, 1631. (c) Han, J. W.; Hill, C. L. *J. Am. Chem. Soc.* **2007**, *129*, 15095. (d) Yu, K.; Zhou, B.-B.; Yu, Y.; Su, Z.-H.; Yang, G.-Y. *Inorg. Chem*. **2011**, *50*, 1862.

(9) (a) Zheng, S.-T.; Zhang, J.; Yang, G.-Y. *Angew. Chem. Int. Ed*. **2008**, *47*, 3909. (b) Miras, H. N.; Vilà-Nadal, L.; Cronin, L. *Chem. Soc. Rev*. **2014**, *43*, 5679.

(10) Wang, S.-S.; Yang, G.-Y. *Chem. Rev*. **2015**, *115*, 4893.

(11) (a) Keita, B.; Nadjo, L. *J. Mol. Catal. A : Chemical* **2007**, *262*, 190. (b) Keita, B.; Kortz, U.; Bruna Holzle, L. R.; Brown, S.; Nadjo, L. *Langmuir* **2007**, *23*, 9531. (c) Hijazi, A.; Kemmegne-Mbouguen, J. C.; Floquet, S.; Marrot, J.; Fize, J.; Artero, V.; David, O.; Magnier, E.; Pégot, B.; Cadot, E. *Dalton Trans*. **2013**, *42*, 4848. (d) Von Allmen, K.; More, R.; Mueller, R.; Soriano-Lopez, J.; Linden, A.; Patzke, G. R. *ChemPlusChem*. **2015**, *80*, 1389.

(12) Oms, O.; Dolbecq, A., Mialane, P., *Chem. Soc. Rev.* **2012**, *41*, 7497

(13) Rousseau, G.; Zhang, S.; Oms, O.; Dolbecq, A.; Marrot, J.; Liu, R.; Shang, X.; Zhang, G.; Keita, B.; Mialane, P. *Chem. Eur. J.* **2015**, *21*, 12153.

(14) (a) Lv, H.; Geletii, Y. V.; Zhao, C. ; Vickers, J. W. ; Zhu, G. ; Luo, Z. ; Song, J. ; Lian, T. ; Musaev, D. G. ; Hill, C. L. *Chem. Soc. Rev*. **2012**, *41*, 7572. (b) Lee, C.-Y.; Guo, S.-X.; Murphy, A. F.; McCormac, T.; Zhang, J.; Bond, A. M.; Zhu, G.; Hill, C. L.; Geletii, Y. V. *Inorg. Chem*. **2012**, *51*, 11521. (c) Evangelisti, F.; Car, P.-E.; Blacque, O.; Patzke, G. R. *Catal. Sci. Techn*. **2013**, *3*, 3117.

(15) Kibsgaard, J.; Jaramillo, T. F.; Besenbacher, F. *Nature Chem*. **2014**, *6*, 248.

(16) Chen, W.-F. ; Muckerman, J. T.; Fujita, E. *Chem Commun*. **2013**, *49*, 8896.

(17) (a) Simmons, T. R.; Berggren, G.; Bacchi, M.; Fontecave, M.; Artero, V. *Coord. Chem. Rev*. **2014**, *270-271*, 127. (b) DuBois, D. L.; Bullock, R. M. *Eur. J. Inorg. Chem*. **2011**, 1017.

(18) Porcher, J.-P.; Fogeron, T.; Gomez-Mingot, M.; Derat, E.; Chamoreau, L.-M.; Li, Y.; Fontecave, M. *Angew. Chem. Int. Ed*. **2015**, *54*, 14090

(19) Chen, J.; Huang, J.; Swiegeres, G. F.; Too, C. O.; Wallace, G. G. *Chem. Commun*. **2004**, 308.

(20) Queyriaux, N.; Jane, R. T.; Massin, J.; Artero, V.; Chavarot-Kerlidou, M. *Coord. Chem. Rev.* **2015**, *304-305*, 3.

(21) Jain, A.; Lense, S.; Linehan, J. C.; Raugei, S.; Cho, H.; DuBois, D. L.; Shaw, W. J. *Inorg. Chem*. **2011**, *50*, 4073.

(22) (a) Chambers, M. B.; Wang, X.; Elgrishi, N.; Hendron, C. H.; Walsh, A.; Bonnefoy, J.; Canivet, J.; Quadrelli, E. A.; Farrusseng, D.; Mellot-Draznieks, C.; Fontecave, M. *ChemSusChem*. **2015**, *8*, 603. (b) Kajiwara, T.; Fujii, M.; Tsujimoto, M.; Kobayashi, K.; Higuchi, M.; Tanaka, K.; Kitagawa, S. *Angew. Chem. Int. Ed. Engl*. **2016**, *55*, 2697. (c) Maza, W. A.; Padilla, R.; Morris, A. J. *J. Am. Chem. Soc*. **2015**, *137*, 8161. (d) Kim, D.; Whang, D. R.; Park, S. Y. *J. Am. Chem. Soc*. **2016**, 138, 8698. (e) Hou, C.-C.; Li, T.-T.; Cao, S.; Chen, Y.; Fu, W.-F. *J. Mat. Chem. A* **2015**, *3*, 10386.

(23) (a) Nohra, B.; El Moll, H.; Rodriguez Albelo, L. M.; Mialane, P.; Marrot, J.; Mellot-Draznieks, C.; O'Keeffe, M.; Ngo Biboum, R.; Lemaire, J.; Keita, B.; Nadjo, L.; Dolbecq, A. *J. Am. Chem. Soc*. **2011**, *133*, 13363. (b) Rousseau, G.; Rodriguez-Albelo, L. M. ; Salomon, W. ; Mialane, P. ; Marrot, J. ; Doungmene, F. ; Mbomekallé, I.-M. ; de Oliveira, P. ; Dolbecq, A. *Cryst. Growth Des*. **2015**, *15*, 449. (c) Qin, J.-S.; Du, D.-Y.; Guan, W.; Bo, X.-J.; Li, Y.-F.; Guo, L.-P.; Su, Z.-M.; Wang, Y.-Y.; Lan, Y.-Q.; Zhou, H.-C. *J. Am. Chem. Soc*. **2015**, *137*, 7169.

(24) Rodriguez-Albelo, L. M.; Ruiz-Salvador, A. R.; Sampieri, A.; Lewis, D. W.; Gómez, A.; Nohra, B.; Mialane, P.; Marrot, J.; Sécheresse, F.; Mellot-Draznieks, C.; Ngo Biboum, R.; Keita, B.; Nadjo, L.; Dolbecq, A. *J. Am. Chem. Soc.* **2009**, *131*, 16078.

(25) Rodriguez Albelo, L. M.; Rousseau, G.; Mialane, P.; Marrot, J.; Mellot-Draznieks, C.; Ruiz-Salvador, A. R.; Li, S.; Liu, R.; Zhang, G.; Keita, B.; Dolbecq, A. *Dalton Trans*. **2012**, *41*, 9989.

(26) Rodriguez Albelo, L. M. ; Ruiz-Salvador, A. R. ; Lewis, D. W. ; Gómez, A. ; Mialane, P. ; Marrot, J. ; Dolbecq, A. ; Sampieri, A. ; Mellot-Draznieks, C. *Phys. Chem. Chem. Phys*. **2010**, *12*, 8632.

(27) Miao, H. ; Hu, G. ; Guo, J. ; Wan, H. ; Mei, H. ; Zhang, Y. ; Xu, Y. *Dalton Trans*. **2015**, *44*, 694.

(28) (a) Lei, C. ; Mao, J. G. ; Sun, Y. Q. ; Song, J. L. *Inorg. Chem*. **2004**, *43*, 1964. (b) Dolbecq, A. ; Mellot-Draznieks, C. ; Mialane, P. ; Marrot, J. ; Férey, G. ; Sécheresse, F. *Eur. J. Inorg. Chem*. **2005**, 3009.

(29) Fu, H.; Qin, C.; Lu, Y.; Zhang, Z.-M.; Li, Y.-G.; Su, Z.-M.; Li, W.-L.; Wang, E.-B. *Angew. Chem. Int. Ed.* **2012**, *51*, 7985.

(30) (a) Guo, S.-X.; Lee, C.-Y.; Zhang, J.; Bond, A. M.; Geletii, Y. V.; Hill, C. L. *Inorg. Chem*. **2014**, *53*, 7561. (b) Yin, Q. S.; Tan, J. M.; Besson, C.; Geletii, Y. V.; Musaev, D. G.; Kuznetsov, A. E.; Luo, Z.; Hardcastle, K. I.; Hill, C. L. *Science* **2010**, *328*, 342. (c) Zhang, C.; Lin, X.; Zhang, Z.; Long, L.-S.; Wang, C.; Lin, W. *Chem. Commun*. **2014**, *50*, 11591.

(31) (a) Kim, J.; Chen, B.; Reineke, T. M.; Li, H.; Eddaoudi, M.; Moler, D. B.; Keeffe, M. O.; Yaghi, O. M. *J. Am. Chem. Soc.* **2001**, *4*, 8239. (b) Inorganic Synthesis, 1990, volume 28, 338, Wiley and Sons Eds.

(32) Sheldrick, G. M. SADABS, program for scaling and correction of area detector data, University of Göttingen, Germany, 1997.

(33) Blessing, R. *Acta Crystallogr.* **1995**, *A51*, 33.

(34) Sheldrick, G. M. SHELX-TL version 5.03, Software Package for the Crystal Structure Determination, Siemens Analytical X-ray Instrument Division : Madison, WI USA, 1994.

(35) van der Sluis, P.; Spek, A. L. *Acta Crystallogr., Sect. A.* **1990**, *46*, 194.

(36) See for example (a) Maniam, P.; Stock, N. *Inorg. Chem.* **2011**, *50*, 5085. (b) Devic, T.; Serre, C.; Audebrand, N.; Marrot, J.; Férey, G. *J. Am. Chem. Soc*. **2005**, *127*, 12788. (c) Chae, H. K.; Siberio-Pérez, D. Y.; Kim, J.; Go, Y. ; Eddaoudi, M.; Matzger, A. J.; O'Keeffe, M.; Yaghi, O. M. *Nature* **2004**, *427*, 523.

(37) Dong, B.-X.; Chen, L.; Zhang, S.-Y.; Ge, J.; Song, L.; Tian, H.; Teng, Y.-L; Liu, W.-L. *Dalton Trans.* **2015**, *44*, 1435.

(38) Kuleska, P. J.; Chojak, M.; Miecznikowski, K.; Lewera, A.; Malik, M. A.; Kuhn, A. *Electrochem. Commun*. **2002**, *4*, 510.

(39) (a) Kulesza, P. J.; Faulkner, L. R. *J. Am. Chem. Soc.* **1988**, *110*, 4905. (b) Kulesza, P. J.; Faulkner, L. R. *J. Electroanal. Chem. Interfacial Electrochem.* **1988**, *248*, 305. (c) Kulesza, P. J.; Faulkner, L. R. *J. Electroanal. Chem. Interfacial Electrochem.* **1989**, *259*, 81. (d) Kulesza, P. J.; Lu, W.; Faulkner, L. R. *J. Electroanal. Chem.* **1992**, *336*, 35.

(40) Zhang, C.; Hong, Y.; Dai, R.; Lin, X.; Long, L.-S.; Wang, C.; Lin, W. *ACS Appl. Mater. Interfaces* **2015**, *7*, 11648.

(41) Walter, M. G.; Warren, E. L.; McKone, J. R.; Boettcher, S. W.; Mi, Q.; Santori, E. A.; Lewis, N. S. *Chem. Rev*. **2010**, *110*, 6446.

FOR TABLE OF CONTENTS USE ONLY

Effect of Cations on the Structure and Electrocatalytic Response of Polyoxometalate-Based Coordination Polymers

William Salomon,[†] Grégoire Paille,[†,‡] Maria Gomez-Mingot,*[,‡] Pierre Mialane,[†] Jérôme Marrot,[†] Catherine Roch-Marchal,[†] Gregory Nocton,[§] Caroline Mellot-Draznieks,[‡] Marc Fontecave,*[,‡] and Anne Dolbecq*[,†]

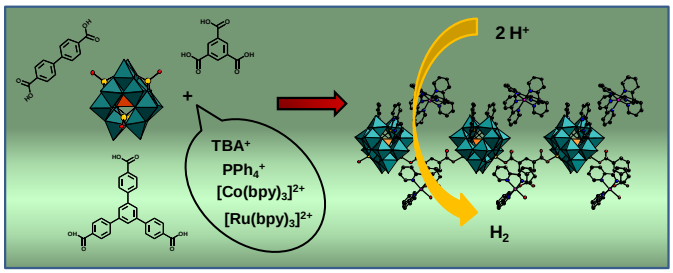

The structure of polyoxometalate-based coordination polymers has been modulated from 1D to 3D by using di- or tri-carboxylate linkers and various counter-ions. The catalytic H_2 production by controlled potential electrolysis of these materials depends on the nature of the counter-ions.